Journal of Thermal Biology 80 (2019) 45–55

Contents lists available at ScienceDirect

Journal of Thermal Biology

journal homepage: www.elsevier.com/locate/jtherbio

A numerical-experimental study on thermal evaluation of orthodontic tooth movement during initial phase of treatment

M. Fakhimi Bonab[a], A. Mojra[a,*], M. Shirazi[b]

[a] Department of Mechanical Engineering, K. N. Toosi University of Technology, 15 Pardis St., Tehran 1991943344, Iran
[b] Department of Orthodontics and Dental Research Centre, School of Dentistry, Tehran University of Medical Sciences, Tehran, Iran

ARTICLE INFO

Keywords:
Orthodontic treatment
Thermal analysis
Pennes bio-heat transfer equation, Hyper-viscoelastic behavior
Finite element method

ABSTRACT

The most desired target of orthodontic treatment is tooth movement as a result of application of efficient force system. In this study, effect of tooth loading is studied on temperature profile around the tooth at early stages of treatment. The basis of temperature variation is increase of cell number and activities in periodontium as a result of compression and tension of this layer. Highest cellular activities occur in the beginning of loading procedure and aim to reduce mechanical stress in the periodontium which finally ends up with orthodontic tooth movement during couple of years. To find out the correlation between temperature variation and the applied force, in vivo experiments are conducted on ten rats and temperature is measured in specific time periods. It is observed that temperature is higher in direction of the net force about 0.3°C. Next, numerical finite element analysis is carried out on the rat tooth model. Mechanical stress results show that regions with compressive stress have rather high temperature in the experiments. Mechanical stress on periodontium-bone interface is multiplied by a coefficient to simulate cellular activities on this boundary as a heat source and thermal analysis is carried out to obtain temperature profile. The thermo-mechanical coefficient is identified for each rat by imposing the experimental temperatures on numerical outputs. For assessment of a treatment efficiency and deduction of the applied force, temperatures could be measured experimentally and compared with the corresponding numerical analysis temperature result obtained by employing the thermo-mechanical coefficient found earlier for each rat.

1. Introduction

Orthodontics is the skill of fixing tooth displacement which could appear as translation, rotation, extrusion or intrusion in different sides of a tooth (Li et al., 2014; Nakajima et al., 2007). Orthodontic treatment is performed practically by applying force on the tooth crown. In this procedure, four factors of magnitude, type (for bodily transformation and rotation of the tooth), direction and location of the force are adjusted based on the desirable tooth displacement. Orthodontic treatment is a time-consuming process and it cannot be evaluated in the early stages; therefore, any misapplication of each factor can lead to irreparable damages and can hamper the orthodontic procedure (Danz et al., 2016; Ammar et al., 2011; Dorow and Sander, 2005).

In order to prevent probable mistakes, several numerical studies have been conducted to investigate the influence of different loadings in order to accurately estimate the required force for an appropriate displacement. Liao et al. (2016) applied a wide range of force magnitudes on a model of the human maxillary teeth. They obtained the center of resistance and the optimal orthodontic force through hydrostatic stress measurement in the periodontal ligament (PDL) which is a connective soft tissue around the tooth. They concluded that when a major proportion of the tooth is under stress, orthodontic process would be more effective. In order to determine the proper loading, instead of using the moment to force ratio, the location of center of resistance was announced as an appropriate factor in determining the treatment process (Liao et al., 2016).

Numerical simulation can greatly improve the effectiveness of dental procedure. However, similar to the practical treatment, being time-consuming is one of the fundamental difficulties in the mechanical simulations of an orthodontic treatment. There are a number of attempts in the literature for long-term simulations. Zargham et al. Zargham et al. (2016) did a long-term simulation and studied tooth movement, rotation and bone loss in a four-week period while the tooth was under specific loading condition. In this study, elastic property was considered for all components of the tooth. At each iteration, geometry and mesh were updated from the last iteration. Rather than the numerical costs, long-time loading of the tooth has some consequences including enamel declassification, tooth decay and root resorption

* Corresponding author.
E-mail addresses: fakhimi.mehdi@email.kntu.ac.ir (M.F. Bonab), mojra@kntu.ac.ir (A. Mojra), shirazi_m@tums.ac.ir (M. Shirazi).

https://doi.org/10.1016/j.jtherbio.2019.01.005
Received 28 August 2018; Received in revised form 2 January 2019; Accepted 6 January 2019
Available online 08 January 2019
0306-4565/

(Sameshima and Sinclair, 2001). These consequences affect the geometry and mechanical properties during the simulation and reduce accuracy of the results. Therefore, long-term evaluation of the orthodontic treatment has inevitable problems both numerically and practically.

The main objective of the present study is to focus on an early evaluation method based on temperature variation around the tooth structure as a result of appliance insertion. Detailed explanation of fundamentals of this method can be found in the work of Heidary et al. (2018). In this study, in vivo experiments are performed on ten Wistar rats and thermal parameters are measured in two time periods; in two weeks of load insertion on the first maxillary molar tooth and two subsequent weeks of load removal. Meanwhile, a thermo-mechanical finite element analysis (FEM) is conducted on the rat's tooth model which is constructed by a section of micro-CT scan images. For a reliable numerical simulation, the geometry and the mechanical properties of the tooth components should be defined precisely. To this end, the tooth structure is modeled by considering three components of the tooth, PDL and the alveolar bone. Material properties of the bone and the tooth are defined according their elastic behavior (Kawarizadeh et al., 2003).

Unlike the bone and the tooth, the PDL has a complex structure and behavior (Jiang et al., 2016). It plays a determining role in the orthodontic procedure (Christopher et al., 2000). In spite of inaccurate and limited information about the PDL, researchers have tried to simulate mechanical behavior of this tissue in different ways. Many previous studies have simulated the PDL as a linear elastic material. Cai et al. (2015) conducted a 3D finite element modeling on canine's tooth to study stresses in the canine's PDL during canine's translation, inclination, and rotation. They considered an elastic behavior for the periodontium and observed that stresses in the PDL were exponential in transparent tooth correction treatment. Provatidis (Provatidis, 2000) studied different mechanical representations of the PDL and their effects on the tooth mobility. The PDL was considered as linear and nonlinear elastic materials while isotropic, anisotropic and orthotropic orientations were considered for the constitutive fibers. FEM was used to estimate the occlusal positions on the maxillary central incisor. Viecilli et al. Viecilli and Burstone (2015) produced a finite element model of all teeth and applied four different types of loads. They calculated the third principal stresses of different teeth in areas of most compression while the PDL was assumed as a linear elastic material. Based on the results, resistance numbers representative of the load proportions for each tooth were determined. Bouton et al. Bouton et al. (2017) developed a finite element (FE) analysis to evaluate stresses and their distribution on the level of the tooth, the elastic PDL and the alveolar bone when a force is applied. They could monitor the tooth movement by obtaining optical impressions at each stage of treatment. FE analyses were correlated with the clinically-observed displacement.

However, according to the tissue structure, elastic assumption could not properly characterize the tissue behavior (McCormack et al., 2014; Toms et al., 2002). PDL has a fibrous structure which causes a nonlinear mechanical response of the soft tissue. It also acts as a damper when it is confronted with mechanical stress which results in time-dependent responses (Heidary et al., 2018; Storey, 1973). In some studies, hyperelastic property has been considered for nonlinear variations of mechanical stress and strain in the PDL. However, viscoelastic property can best characterize the nonlinear behavior of stress and strain with regard to the time (Qian et al., 2009; Su et al., 2013; Maruo et al., 2016; Oskui and Hashemi, 2016).

The main role of the PDL is providing space for bone cells accumulation. Osteoblasts and osteoclasts are two types of cells that exist near the bone layer in the PDL tissue. These cells play a significant role in orthodontics displacement and are sensitive to the mechanical stress. By applying force to the tooth crown, osteoclast cells accumulate in the regions where the compressive stress exists and destroy the bone tissue on the common surface between the PDL and the alveolar bone (Kawarizadeh et al., 2003). Afterwards, osteoblast cells are activated in the regions with tensile stress (Kawarizadeh et al., 2003). Therefore, by analyzing the mechanical compressive stress in the PDL, erosion of the alveolar bone could be estimated and that is where orthodontics process is believed to initiate (Field et al., 2009).

Osteoblast cells generate extra heat in the periodontium during metabolic process which is referred to as metabolic heat. Amount of the metabolic heat depends on the number of osteoclast cells which has correlation with the value of compressive stress. The extra metabolic heat affects normal temperature distribution in the tooth structure and gives rise to the temperature in the regions of compressive stress which depends on the direction of the applied force to the tooth. To find out the correlation between the applied force and the corresponding temperature rise, the profile of temperature variation in the experimental study are equalized with the temperature outputs in the numerical study and the required thermal conditions are estimated. The acquired thermal condition provides the coupling between mechanical stress and temperature values.

2. Material and methods

2.1. Problem definition

The desired target of orthodontic treatment is tooth movement as a result of application of efficient force system. Orthodontic tooth movement takes a long time therefore the inefficiency cannot be early detected. In the present study, temperature variation is measured around the tooth structure after a few weeks of load insertion on the tooth crown. The main objective is to find a correlation between the applied force and the temperature profile.

The reason for temperature rise is increase of cell numbers and cellular activities in the periodontium during tooth loading which aims to reduce the compressive and tensile stresses resulted from force insertion on the tooth. By reducing the mechanical stress, the temperature gradient vanishes and finally ends up with the occurrence of orthodontic tooth movement. Therefore, thermal measurements are more effective in the early stages of appliance insertion.

To find out the correlation between force and temperature, first an experimental study is carried out on rats and temperature is measured while the tooth is loaded for a specific period of time (two weeks). In the next step, a mechanical analysis is conducted for the tooth model and mechanical stress distribution is obtained and compared with experimental temperature profile. The force-temperature correlation is finally found out by doing a thermal analysis on the tooth model with the aim of attaining temperature results similar to the experiments. Once the force-temperature relevance is known for each rat, the orthodontic treatment could be assessed. To do so, temperature is measured experimentally in a new condition at a specific time; meanwhile, the numerical analysis is conducted similar to the experiment and temperature is obtained based on the force-temperature relationship identified earlier for each rat. Comparison between the numerical and experimental temperatures could be used for deduction of the applied force and assessment of treatment efficiency at that particular time.

2.2. Experiment

2.2.1. Experimental protocol

The experimental tests are conducted on ten male Wistar rats in the pharmacology department of Tehran University, Tehran, Iran. The rats weigh 180–200 gr. All the rats are kept in similar test room and physiological conditions, prior to and during the experiments. Prior to the experiments, the rats have been kept in thermal condition of 22 °C and 12 h light/dark cycle. A 60 gr (0.58 N) force is applied to the first maxillary left molar tooth in the mesial direction of each sample (Fig. 1). The force is exerted by an appliance which is made of 6 mm nickel-titanium closed-coil spring (Niti, 3 M unitek, Monorova, Claif,

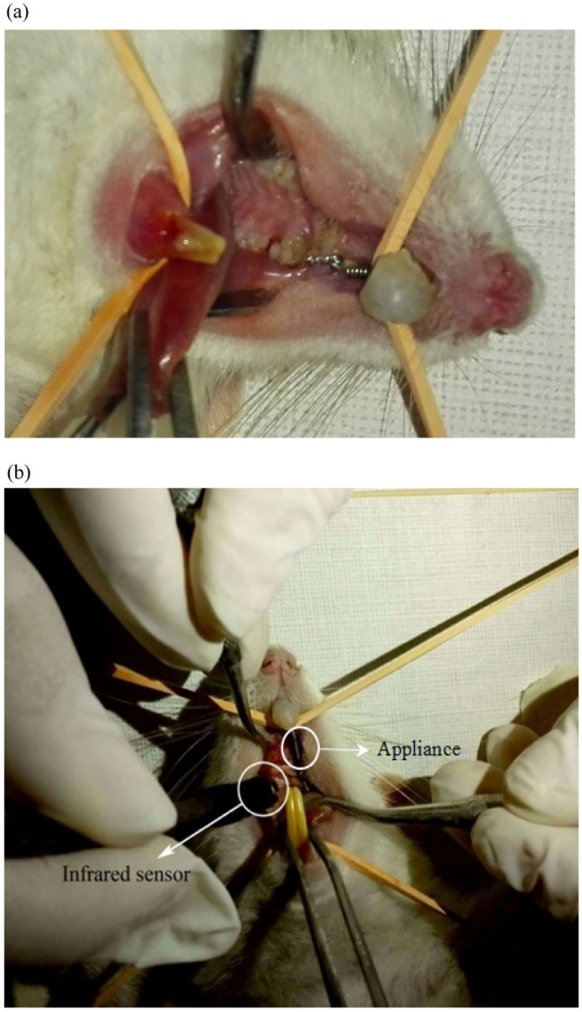

Fig. 1. (a) Appliance is inserted on the first left maxillary molar tooth in the mesial direction; (b) temperature measurement is performed by an infrared sensor in three directions of palatal, mesial and buccal for the left and the right maxillary molar teeth (Heidary et al., 2018).

Hitek 0.006 × 0.022 in) and a ligature wire (0.001 in). The force is measured by a force gauge.

Temperature is measured in two periods of time. The first measurement is performed after two weeks of appliance insertion. In the next phase, the appliance is removed and the temperature is measured again after two more weeks.

Every tooth has four lateral surfaces which are palatal, buccal, mesial and distal (Fig. 2). Buccal and palatal are the nearest surfaces to the cheek and to the tongue, respectively; while mesial and distal are surfaces in contact with other adjacent teeth. Mesial is toward the front of the mouth while distal is toward the back.

For each rat, temperature is measured on three surfaces in three directions of buccal, palatal, and mesial. In order to identify the effect of the applied force on temperature variation, temperature is measured in similar directions of the right maxillary molar tooth which is not loaded by an appliance.

2.2.2. Experimental setup

The temperature is measured by a non-contact infrared thermal sensor, MLX90615. SSG-DAx. Features of this sensor are presented in Table 1 according to MLX90615 Melexis factory datasheet. According to the size, response time and accuracy of measurement in the range of 0–40 °C, this sensor could be used for medical applications. With regard to the lack of access to the periodontium layer, temperature is measured on the gum in proximity to the root.

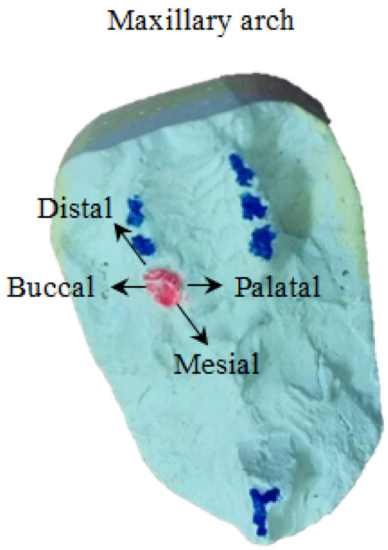

Fig. 2. Lateral surfaces of the first maxillary molar tooth of a rat (colored in red).

Table 1
MLX features according to MLX90615 Melexis factory datasheet, data are in °C.

Sensor	Resolution	Accuracy	Range of ambient temperature	Range of object temperature
MLX	0.02	0.2–0.3	16–40	32–42

It should be mentioned that the temperature drops on the gum relative to the periodontium. Since the basis of treatment evaluation in this study is the temperature elevation as a result of load application, lower temperatures do not have impact on the validity of the results.

2.3. Numerical study

2.3.1. Geometry construction

The model of the first maxillary molar tooth of a rat is constructed by using a section of micro-CT images. Images are imported to the Mimics software (version 10.01) and the geometrical model is created by importing the Mimics output to the SOLIDWORKS software (version 2016) (Fig. 3a).

The resultant geometry is simplified in the buccopalatal direction by neglecting geometrical complexities of the mesial and the distal surfaces to avoid excessive increase in the computational time and to solve the problem with an efficient approach. 3D geometry is constructed by extruding the geometry of buccal surface along the normal direction by 1 mm. Geometry of the buccal surface is constructed by using the CT images. The PDL and bone layers are created through a 0.12 mm offset of the tooth surfaces in the mesial and distal directions (Cuoghi et al., 2013).

2.3.2. Governing equations and material properties

The tooth structure is a thermal system which consists of different thermal terms including blood perfusion and metabolic heat generation. In the orthodontic treatment, performance of the thermal system is affected by load insertion which affects the tooth normal temperature. The Pennes bio-heat transfer equation (Eq. (1)) is used for heat transfer in the periodontium tissue (Oskui and Hashemi, 2016).

$$\rho C_p \frac{\partial T}{\partial t} = k\left(\frac{\partial^2 T}{\partial x^2} + \frac{\partial^2 T}{\partial y^2} + \frac{\partial^2 T}{\partial z^2}\right) + \eta_b \rho_b C_{pb}(T_a - T) + Q_m + Q_s \quad (1)$$

where, C_p is specific heat of the tissue, η_b is blood perfusion rate, C_{pb} is

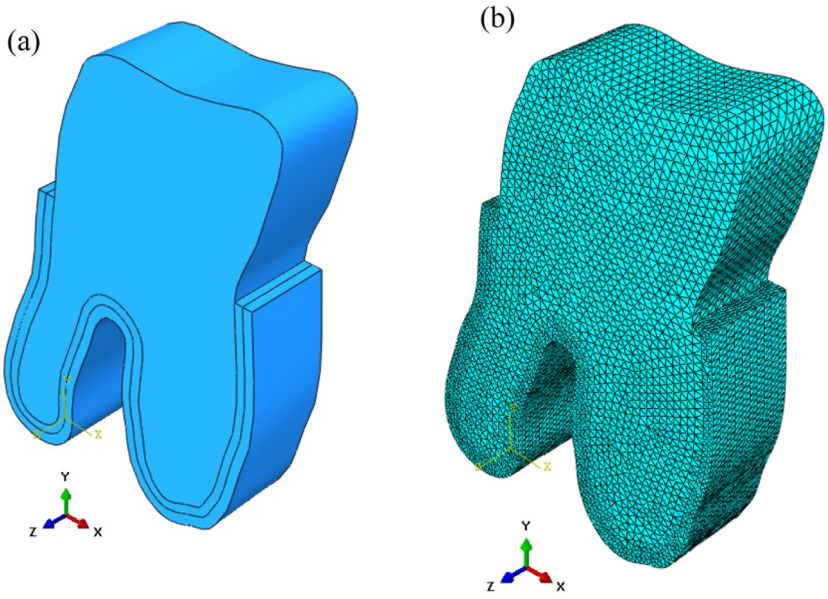

Fig. 3. (a) Geometrical model of the rat tooth, (b) meshed geometry with coupled temperature-displacement elements in ABAQUS software.

Table 2
Mechanical and thermal properties of the tooth and the alveolar bone (Su et al., 2013; Er et al., 2007).

Tissue	Modulus of Elasticity (MPa)	Poisson's ratio	Density (g/mm3)	Thermal conductivity (J/mm.s.∘C)	Specific heat (J/g.∘C)
tooth	18,600	0.31	4E-3	6.2805E-04	1.17236
bone	13,700	0.3	1.3E-3	5.8618E-04	1.84228
PDL	–	–	1E-3	5.8618E-04	4.817

specific heat of the blood, ρ is the tissue density, k is thermal conductivity, ρ_b is density of the blood, Q_m is metabolic heat generation, Q_s is distributed volumetric heat source due to spatial heating, t is time, T is temperature, and T_a is temperature of the artery. In the present study, effect of blood perfusion is neglected and the there is no spatial heat source. Thermal properties of the tooth, PDL and the bone can be found in Table 2.

For the mechanical properties, the tooth and the alveolar bone are defined as homogeneous elastic materials (Su et al., 2013). The compressive stress in these layers is determined with the following equation (Eq. (2)):

$$\sigma_{compressive} = -\frac{1}{3}\sum_{i=1}^{3}\sigma_{ii} \tag{2}$$

where σ_{11}, σ_{22}, and σ_{33} are the first, second, and third principal stresses, respectively, E is the modulus of elasticity and ε is the strain. Thermal and mechanical properties of the elastic components are presented in Table 2.

In order to define the PDL properties, visco-hyperelastic model is considered based on the nonlinear and time-dependent behavior of the tissue. This model considers both hyperelastic and viscoelastic responses which are related to the nonlinear and time-dependent behaviors of the tissue, respectively. More discussion on the PDL modeling can be found in (Heidary et al., 2018; Su et al., 2013). Relevant properties of the viscoelastic and the hyperelastic behavior of PDL tissue are provided in Table 3.

Parameters listed in Table 3 are related to the governing equations of the hyperelastic and the viscoelastic behaviors of the periodontium. The basic formulation for linear isotropic viscoelasticity can be written as Eq. (3), which is an expression of the nonlinear stress-time relation:

Table 3
Hyperelastic and viscoelastic related parameters for defining the PDL mechanical response (Su et al., 2013).

Model	Parameters		
hyperelastic	N	C_{i0}	D_i
	1	0.01	2
	2	5	0.01
	3	1000	0.001
viscoelastic	τ	K	G
	0.0025	0.155	0
	0.1	0.4	0
	0.5	0.15	0

$$\sigma(t) = \int_0^t 2G(t-\mathrm{T})\dot{e}(\mathrm{T})d\mathrm{T} + \mathrm{I}\int_0^t K(t-\mathrm{T})\dot{\varphi}(\mathrm{T})d\mathrm{T} \tag{3}$$

Where here $G(t)$ is the stress relaxation shear modulus, $\dot{e}$ is the rate of change of deviatoric strains, $K(t)$ is the stress relaxation bulk modulus, and $\dot{\varphi}$ is the rate of change of volumetric strains.

$K(t)$ and $G(t)$ can be defined individually in terms of a series of exponentials known as the Prony series (Eqs. (4) and (5)):

$$K(t) = K_\infty + \sum_{i=1}^{M} K_i exp\left(-\frac{t}{\tau_i}\right) \tag{4}$$

$$G(t) = G_\infty + \sum_{i=1}^{M} G_i exp\left(-\frac{t}{\tau_i}\right) \tag{5}$$

Where K_∞ and G_∞ represent the long-term bulk and shear moduli. τ_i is the i^{th} relaxation time. A real material may not relax with a single

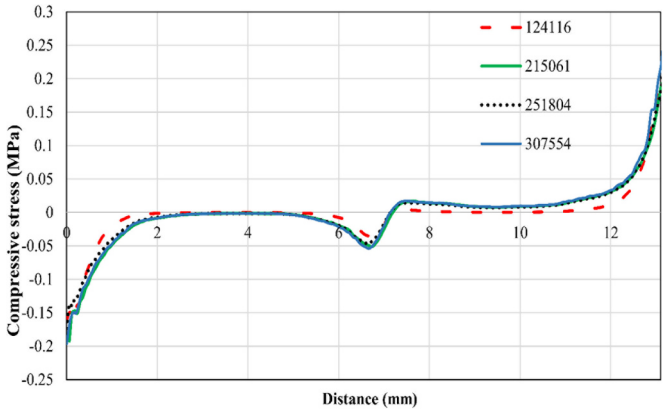

Fig. 4. The compressive stress curve on the PDL-bone interface line for 4 grids with 124116, 215,061, 251,804, and 307,554 elements.

relaxation time due to its molecular structure. M is the number of relaxation times for that material and K_i and G_i are bulk and shear moduli at τ_i.

For the hyperelastic modeling, reduced form of the strain energy function in the polynomial form is used (Eq. (6)):

$$U = \sum_{i=1}^{N} C_{i0}(\bar{I}_1-3)^i + \sum_{i=1}^{N} \frac{1}{D_i}(J-1)^{2i} \quad (6)$$

Where U is the strain energy function, N is the polynomial order, C_{i0} and D_i are the material parameters, J is the elastic volume ratio, and $\bar{I}_1$ is the first deviatoric strain invariant. C_{i0} governs the shear behavior of the material, and D_i determines the compressibility of the material.

2.3.3. Mesh generation and boundary conditions

For the thermo-mechanical analysis, tetrahedral elements by the name of *C3D4T* are used in the ABAQUS software (version 6.13) (Fig. 3b). The elements are selected from the family of Coupled Temperature-Displacement elements.

Mesh independency is checked by studying the compressive stress on a path located on the PDL-bone interface and on the buccal surface. In Fig. 4, the compressive stress is plotted on this path for 4 models with 124116, 215,061, 251,804, and 307,554 elements. The grid with a total number of 124116 elements and 40,732 nodes is accepted because of negligible difference between the curves. For this grid, the tooth is made up of 80178 tetrahedron elements of type *C3D4T*, the PDL consists of 18018 tetrahedron elements of type *C3D4T*, and the alveolar bone consists of 25924 tetrahedron elements of type *C3D4T*.

For the mechanical boundary condition, the tooth, the PDL and the bone are merged together in order to enforce similar mechanical stress and strain on the common surfaces. A concentrated 0.5 N lateral force (Huanga et al., 2012) (in the mesial direction) is applied on the buccal surface to the topmost point of the tooth crown as shown in Fig. 5. The external surfaces which surround the root of the tooth are fixed in all directions. For the thermal boundary condition, initial temperature of 36 °C is considered for the whole model.

Mechanical analysis is performed in the steady state while the thermal analysis is a transient procedure. Both analyses are conducted by the ABAQUS software (version 6.13). Parameters of the transient analysis are listed in Table 4.

The output of mechanical analysis is mechanical stress distribution on the common surface between the periodontium and the bone. The compressive part activates the osteoclast cells which try to dissolve the bone tissue to reduce the pressure in the periodontium (Kawarizadeh et al., 2003). The osteoclasts generate extra metabolic heat on the

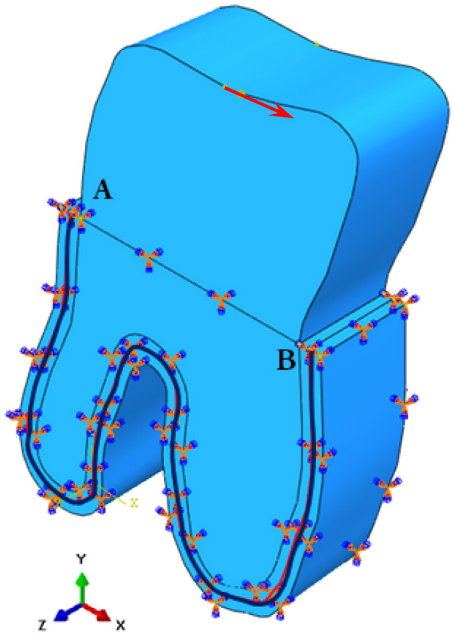

Fig. 5. Mechanical boundary conditions; a path (A-B) is defined on the buccal surface on the boundary between the PDL and the bone.

Table 4
Parameters of the transient thermal analysis; values are in second.

Initial time increment	Minimum time increment	Maximum time increment	Maximum number of increments
0.01	1E-5	1	100

periodontium-bone interface (represents by Q_m in Pennes bio-heat transfer equation provided in Eq. (1)). The amount of heat generation has correlation with the amount of compressive stress and could be identified by obtaining the temperature distribution around the tooth structure similar to the experimental measurements.

3. Results and discussion

3.1. Experimental results

An experimental study is carried out on 10 rats to measure the temperature of the first molar in upper jaw (maxilla). For each rat, temperature is measured in three directions of palatal, buccal and mesial. Due to small size of the maxillary molar tooth and size of the temperature sensor, for each tooth surface only one temperature is reported. Moreover, temperature measurements on the buccal and palatal surfaces are carried out in the vicinity of the mesial surface close to the common edge between mesial and buccal, and mesial and palatal surfaces to study effects of loading on different tooth surfaces. In order to study the effect of loading on the temperature rise, only the left maxillary molar is loaded while measurements are performed for the right and the left maxillary molar teeth.

Temperature measurements and analyzing the temperature rise are performed in specific time periods. A two-week-long period is considered for studying the effect of loading on the temperature rise through appliance insertion on the maxillary left molar tooth. Afterwards the load is removed and temperature measurements are repeated after two more weeks. Table 5 lists the temperature values for

Table 5
Temperature measurements around right and left first maxillary molar teeth by the MLX sensor; measurements are performed in three directions of buccal, palatal and mesial after two weeks of appliance insertion. Data are in ˚C.

Case number	Left (with appliance)			Right (without appliance)			Relative difference (%)		
	Buccal	Palatal	Mesial	Buccal	Palatal	Mesial	Buccal	Palatal	Mesial
1	29.65	30.25	29.40	29.65	29.70	29.10	0.00	1.85	1.03
2	29.46	30.28	30.00	29.30	29.64	29.30	0.55	2.16	2.39
3	28.66	29.22	28.74	28.30	28.88	28.48	1.27	1.18	0.91
4	26.70	26.74	27.00	26.52	26.70	26.60	0.68	0.15	1.50
5	28.52	28.62	28.88	28.52	28.52	28.80	0.00	0.35	0.28
6	28.10	28.52	28.42	27.74	28.34	28.24	1.30	0.64	0.64
7	25.38	26.24	25.80	25.08	25.90	25.08	1.20	1.31	2.87
8	25.62	26.18	25.32	25.56	26.10	25.04	0.23	0.31	1.12
9	26.28	26.86	26.46	26.24	26.76	26.42	0.15	0.37	0.15
10	27.02	27.48	27.24	26.98	27.24	26.84	0.15	0.88	1.49

10 rats in three directions, for both left and right maxillary molar teeth after the first two weeks of loading. Table 6 lists the temperature values for 7 rats along three directions, for both left and right maxillary molar teeth after two weeks of load removal. Relative temperature difference in each direction is calculated by Eq. (7).

$$\textit{Relative temperature difference} = \frac{\textit{Temperature}(\textit{with appliance}) - \textit{Temperature}(\textit{without appliance})}{\textit{Temperature}(\textit{without appliance})} \times 100 \quad (7)$$

In Table 7, temperature differences between similar directions of the left and the right maxillary molar teeth are reported after two weeks of loading and after two weeks of load removal. The absolute temperature difference is calculated according to Eq. (8).

$$\textit{Absolute temperature difference} \quad (^{\circ}C) = \textit{Temperature}(\textit{Left}) - \textit{Temperature}(\textit{Right}) \quad (8)$$

According to Table 1, the resolution of the infrared sensor is 0.02 ˚C; therefore, the amount of temperature rise reported in Table 7 is detectable by the thermal sensor. Temperature measurement around the tooth is a measure of the extent of osteoclast cells accumulation on different surfaces of the tooth. Maximum temperature difference by the end of the 2nd week is up to 4.5, 16, and 40 times greater than the 4th week in the buccal, palatal, and mesial directions, respectively. By removing the load, the temperature drops gradually. According to Table 7, by the end of the 4th week, the temperature gradient is insignificant but there is still slight sign of osteoclasts existence in the vicinity of the tooth.

In order to compare the temperature increase along each direction, relative temperature difference is displayed as a 3D bar chart in Fig. 6. In this figure the horizontal axis represents three temperature values for each rat along three directions after two weeks of appliance insertion. Positive value of relative temperature difference in at least one direction indicates that the temperature is increased as a result of appliance insertion. From this figure the following items could be concluded:

1. For 50% of all cases, temperature elevation is the most in the mesial direction compared to the buccal and the palatal directions which include 20% and 30% of the whole population study, respectively. This output is compatible with the numerical thermal results which mark the highest temperature on the mesial surface relative to the buccal and the palatal surfaces.
2. Maximum relative temperature rise is 2.87%, 1.85% and 1.30% in the mesial, palatal, and buccal directions, respectively.

Table 7
Temperature difference between the first right and left maxillary molar teeth in three directions of buccal, palatal and mesial after two weeks of appliance insertion and two subsequent weeks of appliance removal, data are in ˚C.

Case number	2 weeks of load insertion			2 weeks of load removal		
	Buccal	Palatal	Mesial	Buccal	Palatal	Mesial
1	0.00	0.55	0.30	0.12	0.08	− 0.14
2	0.16	0.64	0.70	− 0.22	0.04	0.10
3	0.36	0.34	0.26	0.08	0.08	0.02
4	0.18	0.04	0.40	0.23	0.08	− 0.01
5	0.00	0.10	0.08	0.16	0.04	0.02
6	0.36	0.18	0.18	–	–	–
7	0.30	0.34	0.72	0.18	− 0.04	0.06
8	0.06	0.08	0.28	–	–	–
9	0.04	0.10	0.04	− 0.12	0.12	0.06
10	0.04	0.24	0.40	–	–	–

Table 6
Temperature measurements repeated after two weeks of the appliance removal, data are in ˚C.

Case number	Left (without appliance)			Right (without appliance)			Relative difference (%)		
	Buccal	Palatal	Mesial	Buccal	Palatal	Mesial	Buccal	Palatal	Mesial
1	29.14	29.46	28.38	29.02	29.38	28.52	0.41	0.27	− 0.49
2	29.96	30.00	29.28	30.18	29.96	29.18	− 0.73	0.13	0.34
3	28.62	28.92	28.72	28.54	28.84	28.70	0.28	0.28	0.07
4	33.55	33.22	32.75	33.06	33.14	32.76	0.70	0.24	− 0.03
5	28.68	29.18	28.44	28.52	29.14	28.42	0.56	0.14	0.07
7	30.28	30.22	29.50	30.10	30.26	29.44	0.60	− 0.13	0.20
9	33.68	34.12	33.02	33.80	34.00	32.96	− 0.36	0.35	0.18

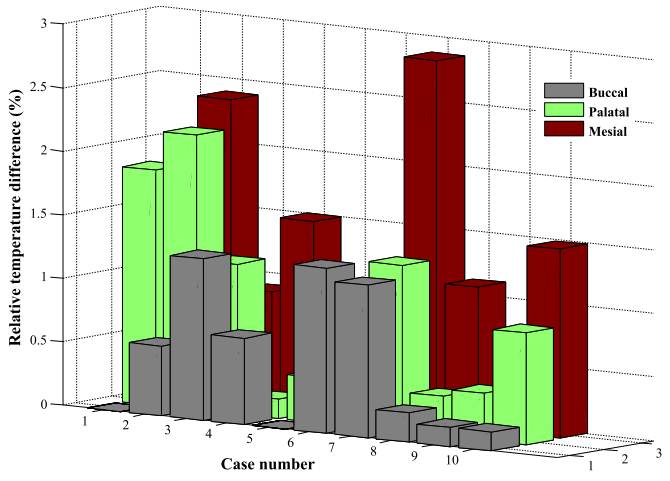

Fig. 6. Relative temperature difference in buccal, palatal, and mesial directions for each of 10 rats, the appliance is inserted on the maxillary left molar tooth and the temperature is measured after two weeks for the left and the right molar teeth.

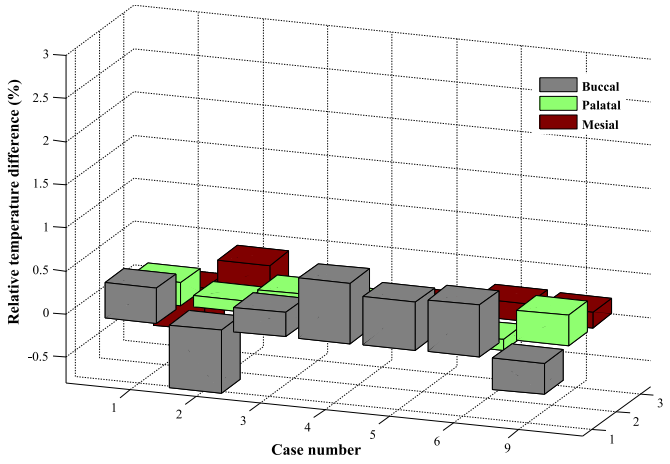

Fig. 7. Relative temperature difference in buccal, palatal, and mesial directions for 7 rats after two weeks passed from the load removal.

3. The measured temperature has wide variation among the rats. The reason can be sought in different elapsed time after induction of anesthesia till the examination time of different rats, and different temperature drop during unconsciousness period for different rats. The latter one causes different initial body temperatures prior to the experiments.

By the end of two-week-long loading period, the appliance is removed. After two more weeks, i.e. by the end of the 4th week, the temperature in three aforementioned directions is measured for both left and right maxillary molar teeth of the rats. In this stage, the tests are conducted on seven rats due to death of cases 6, 8 and 10. Fig. 7 presents the relative temperature differences for seven cases in three directions after two weeks of appliance removal.

A comparison between Figs. 6 and 7 reveals that the relative temperature difference reduces considerably for all cases after 2 weeks of load removal. Maximum relative temperature difference is 0.7% by the end of the 4th week. The mean value of relative temperature difference is 0.15% after two weeks of load removal while it is 0.9% after two weeks of load insertion.

It is noticeable in Figs. 6 and 7 that the temperature has rather wide variations among the rats, especially in the loading procedure. As it has been previously mentioned, the reason can be sought in different elapsed time after induction of anesthesia, induction sequence and the temperature drop after unconsciousness.

In Fig. 8, distribution of the absolute temperature difference in each of buccal, palatal, and mesial directions is displayed for all rats in the first, second, and third columns, respectively. Number of data in each column is 10 in Figs. 8a and 7 in Fig. 8b according to the population study in the loading and load removal procedures. The median of the temperature data along each direction is displayed by a horizontal red line in each column. Medians' location implies that in the mesial direction, data are almost uniformly distributed in both loading and load removal periods among all rats. The opposite can be observed in the buccal direction. The reason can be sought in the location of the buccal surface which is the nearest surface to the cheek and can be easily affected by the environmental temperature. Moreover, as it has been previously noticed, the temperature difference (according to Eq. (8)) has noticeable reduction by the end of the 4th week which remarks the reduction of cellular activities.

The temperature rise in the mesial direction resulted from a 60 gr (0.58 N) force applied on the buccal surface is used to calculate the thermo-mechanical coefficient which correlates the temperature profile to the applied force. This will be reported in the numerical results in Section 3.2.

Two major steps are taken to calculate this coefficient. First Compressive stress is obtained on the PDL-bone interface by applying load to the tooth; second, a heat flux representative of the osteoclast cells' metabolic heat generation is defined on the PDL-bone interface. The pattern of heat flux is similar to the pattern of compressive stress. To identify the amount of heat flux, the compressive stress is multiplied by a thermo-mechanical coefficient. This coefficient is identified in a way that the numerical temperatures become identical with the experimental temperatures for each rat.

According to Table 5, the experimental temperatures have variations among the rats. The reason can be mainly sought in different physiological body response to the applied force, different elapsed time after induction of anesthesia, induction sequence and the temperature drop after unconsciousness.

3.2. Numerical results

3.2.1. Mechanical stress results

Mechanical stress variation is presented for 0.5 N force applied to the topmost point of the first maxillary molar tooth model of a rat (the force has been shown in Fig. 5) similar to the experiments. Fig. 9 displays the compressive stress contour in the tooth, PDL, and the alveolar bone.

It can be inferred from this figure that according to the direction of the applied force, the compressive stress is observed on the mesial surface and on the buccal and palatal surfaces close to the mesial surface while the tensile stress appears on the opposite surface which is the distal. Locations of the maximum compressive and tensile stresses are near the topmost of the root. Studying the profile of mechanical stress shows that regions with high compressive stress are similar to the regions with rather high temperature in the experiments. It could be inferred that force insertion on the tooth crown results in measurable temperature rise.

Analyzing the PDL tissue more specifically, heading from inner layer to outer layer, demonstrates a significant decrease in the compressive stress, which is because of damping property of this layer and is a

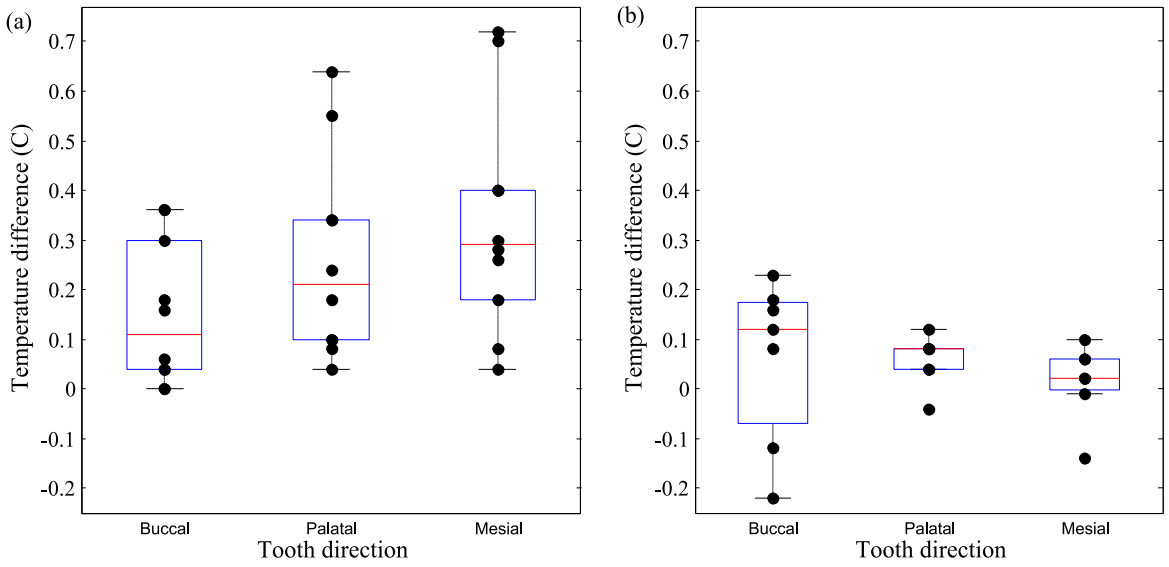

Fig. 8. Distribution of the absolute temperature difference in each of buccal (first column), palatal (second column), and mesial (third column) directions for all rats by the end of (a) second week, and (b) forth week, data are in ℃.

characteristic of viscoelastic materials. This characteristic of the PDL reduces the bone damage during force application. Bone damage includes the fracture or breakage of the bone.

Fig. 10a gives information about the stress distribution on the path A-B which has been shown in Fig. 5. The initial point of the path is at the topmost of the distal surface and the final point is at the topmost of the mesial surface. By a brief glimpse, it can be concluded that the root close to the distal surface is mostly in tension while the other root close to the mesial surface is mostly under pressure. The maximum tensile stress occurs at the start point of the path (point A) and is equal to 0.194 MPa. Meanwhile the maximum compressive stress occurs at the final point of the path (point B) and is equal to 0.25 MPa.

Fig. 10b presents the compressive stress on the PDL-bone common surface. According to the point of force application on the buccal surface, the compressive stress decreases in the buccopalatal direction.

As it was already discussed, the compressive stress triggers the osteoclast cells in the periodontium. The cells accumulate on the PDL-bone interface and try to reduce the pressure by resorption of the bone tissue. For subsequent thermal analysis, cells activity on the PDL-bone interface is considered as a metabolic thermal heat flux. The heat flux has correlation with the compressive stress. As the compression level increases, more cells aggregate to reduce the pressure by dissolving the bone. Therefore, metabolic heat generation and the corresponding heat flux increase as a result of cell aggregation. The heat flux variation on the PDL-bone interface is identical with the pattern of the compressive stress. For periodontium regions with tensile stress, the heat flux is set to zero. This is consistent with the pressure-tension theory which is one of the most important theories of orthodontics. According to this theory, bone resorption (by the osteoclasts) occurs on the side of the PDL where there is pressure. By the end of bone resorption procedure, bone formation (by the osteoblasts) will occur on the opposite side where there is tension.

3.2.2. Thermal results

The aim of thermal analyses is to provide the correlation between the applied force and temperature profile. In the previous section, it has been verified that compressive stress results in detectable temperature rise around the tooth structure. Unlike the mechanical stress, temperature is a measurable quantity in practice; therefore, by finding quantitative correlation between temperature and mechanical stress, performance of load application to the tooth could be evaluated through the study of temperature profile.

The correlation is provided by a coefficient referred to as the thermo-mechanical coefficient. To find out the value of this coefficient, thermal analysis is conducted by applying heat flux to the periodontium-bone interface and the amount of heat flux is obtained by obtaining the temperature distribution similar to the experimental measurements for each rat. The thermo-mechanical is obtained by dividing the amount of heat flux to the compressive stress by considering similar pattern for variation of these variables.

Fig. 11 shows the temperature variation for rat #1 for which the thermo-mechanical coefficient is calculated to be 3.3 by using the aforementioned procedure. As it is expected, the temperature variation is similar to the pattern of compressive stress variation provided in Fig. 10b, e.g. the maximum temperature rise occurs at the topmost region of the buccal surface in which maximum compressive stress is obtained.

According to Fig. 11b, maximum temperature elevation is about 0.3 ℃. Region with enhanced heat transfer has the widest area on the mesial surface compared to the buccal and palatal surfaces.

With regard to variation of temperature values in the experiments for each rat, the obtained thermo-mechanical coefficient is also different for each rat. Table 8 presents the thermo-mechanical coefficient calculated for 10 rats. This coefficient provides the correlation between the mechanical force and the temperature rise. Effectiveness of the treatment could be judged by comparing the desired temperature which can be obtained from numerical analysis and the measured temperature for each case.

It should be mentioned that since the temperature difference is used for evaluating the treatment, results are not biased by normal physiological variations among different rats.

3.3. Simplifications and limitations

In the numerical study, tooth geometry is simplified by neglecting the geometrical complexities of the mesial and distal surfaces. This simplification is made according to the pressure-tension theory which is one of the most important theories of orthodontics. According to this

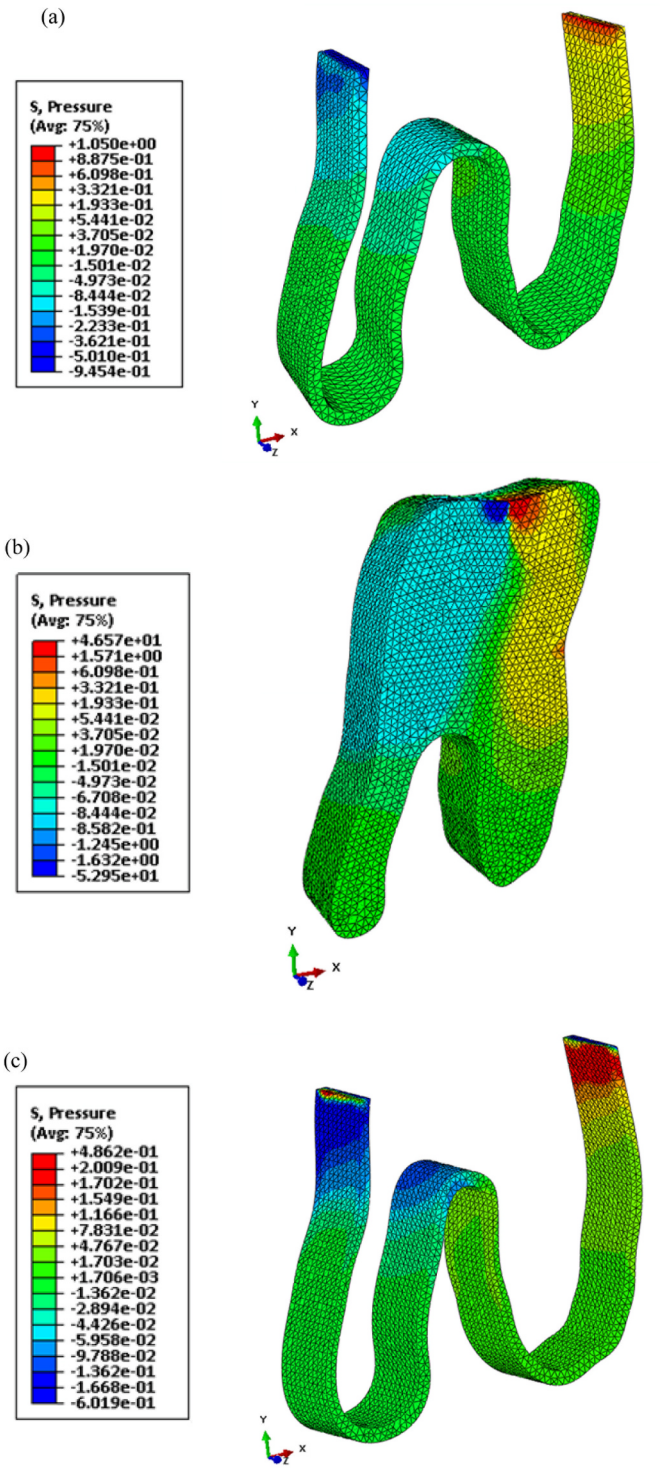

Fig. 9. Compressive stress distribution in (a) the PDL layer, (b) the bone layer, and (c) the tooth; 0.5 N force is applied to the topmost point of the tooth crown on the buccal surface. Data are in MPa.

theory, bone resorption (by the osteoclast) occurs on the side of the PDL where there is pressure. By the end of bone resorption procedure, bone formation (by the osteoblasts) will occur on the opposite side where there is tension.

In this study, according to the direction of the applied force which is the mesiodistal direction, compressive stress appears on the mesial surface and tensile stress appears on the distal surface. Since the point

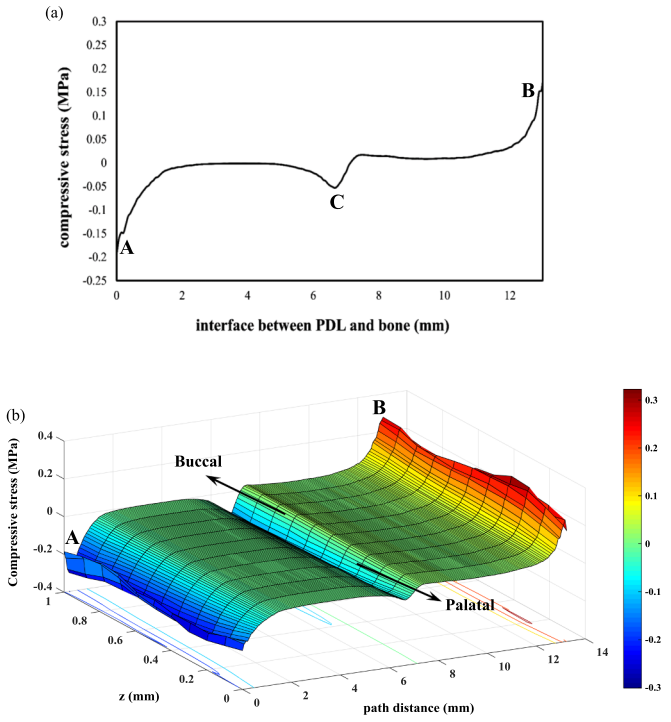

Fig. 10. Compressive stress variation (a) on path A-B, (b) on the common surface between the PDL and the bone; z-direction is along the buccal to the palatal direction and represents thickness of the PDL and the bone (1 mm). A and B are located on the tooth neck and C is located on the root bifurcation. Data are in MPa.

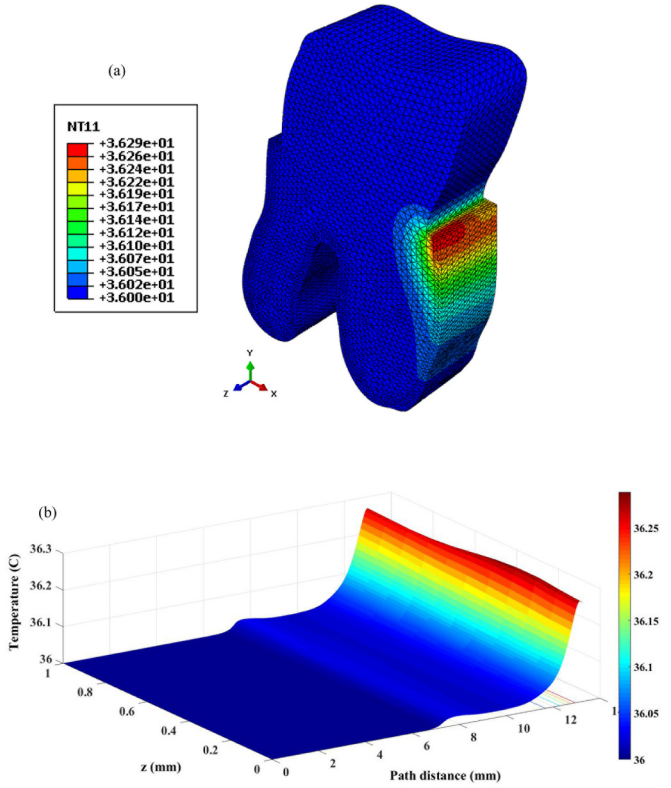

Fig. 11. (a) 3D temperature contour, (b) temperature distribution on the PDL-bone interface resulted from thermal analysis of the tooth model, initial temperature of 36 °C and thermo-mechanical coefficient of "3.3" are assumed. Data are in °C.

Table 8
Thermo-mechanical coefficients for each rat, these coefficients are calculated by imposing the experimental temperatures to the numerical thermal analyses outputs.

Case number	Temperature in the mesial direction (°C) after two-week-long period		Temperature rise (°C)	Thermo-mechanical coefficient (α)
	Right maxillary molar	Left maxillary molar		
1	29.10	29.40	0.30	3.3
2	29.30	30.00	0.70	7.7
3	28.48	28.74	0.26	2.9
4	26.60	27.00	0.40	4.4
5	28.80	28.88	0.08	0.9
6	28.24	28.42	0.18	2.0
7	25.08	25.80	0.72	8.0
8	25.04	25.32	0.28	3.1
9	26.42	26.46	0.04	0.4
10	26.84	27.24	0.40	4.4

of force application is on the buccal surface, therefore, maximum compression and tension appear on the mesial-buccal and distal-buccal common edge. Therefore, discarding the complexity of the third dimension in the buccopalatal direction which includes the mesial and distal surfaces does not have remarkable effect on the results.

From experimental point of view, geometrical simplification is compatible with the experimental limitations. According to the small size of the rat tooth and difficulty in the access to the mesial and the distal surfaces due to the tooth morphology, only one temperature is recorded for each tooth surface. Since calculation of the thermo-mechanical coefficient is based on equalizing the numerical and the experimental temperatures, considering geometrical complexities on the distal and the mesial surfaces does not increase the accuracy of results.

4. Conclusions and future work

In the present study, in vivo experiments are carried out on rats to study effect of an applied force to the tooth crown on temperature variation around the tooth. In the experiments, the first maxillary left molar teeth of 10 rats are loaded by a concentrated force in the mesial direction. Temperature is measured along different directions and comparison is made between the initial values and the corresponding values after two weeks of appliance insertion. It is observed that temperature increases as a result of orthodontic force application. Afterwards, the force is removed and the temperature is measured again after two weeks of load removal and significant temperature reduction is observed. From the experiments, it is concluded that appliance insertion on the tooth, results in measurable temperature rise which is believed to appear due to increased rate of cell activities in the periodontium. In order to correlate force magnitude with the temperature rise, a numerical thermo-mechanical analysis is conducted for the rat tooth model.

Geometrical model of the tooth is constructed based on a section of micro-CT images. The model consists of two elastic layers of the tooth and the alveolar bone and a hyper-viscoelastic layer of periodontium which represents its nonlinear time-dependent response to an applied force. Mechanical analysis is performed in similar loading condition to the experiments. Results indicate that region with compressive stress are equivalent to the regions with rather high temperature in the experiments. This is consistent with the pressure-tension theory in orthodontics which shows higher cell concentration on the bone-periodontium common surface where there is pressure. To find out the quantified correlation between force magnitude and the corresponding temperature rise, a thermal analysis is performed and cellular activity is modeled as a heat flux on the bone-periodontium interface. The heat flux amount is obtained by multiplying the mechanical compressive stress by a thermo-mechanical coefficient for each rat which is attained by imposing the experimental temperature on the numerical thermal output.

By identifying the thermo-mechanical coefficient for each rat, efficiency of an orthodontic treatment could be judged by comparing the desired temperature which can be obtained from numerical analysis and the measured temperature in an in vivo experiment. Moreover, direction of tooth movement could be estimated since temperature rise occurs as a result of the increase of osteoclasts cells accumulation and activities of these cells for reducing the pressure in periodontium by bone resorption, results in orthodontic tooth movement.

Currently, the authors of this article are trying to improve the three-dimensional model of the rat tooth and extend the experimental database for other animals as well as humans with the aim to provide larger space for more accurate thermal measurements.

Funding

This research did not receive any specific grant from funding agencies in the public, commercial, or not-for-profit sectors.

Conflict of interest

The authors declare that they have no conflict of interest.

Ethical approval

This study does not involve human subjects. Institutional guide for the care and use of laboratory animals was followed.

References

Ammar, H.H., Ngan, P., Crout, R.J., Mucino, V.H., Mukdadi, O.M., 2011. Three-dimensional modeling and finite element analysis in treatment planning for orthodontic tooth movement. Am. J. Orthod. Dentofac. Orthop. 139 (1), e59–e71.
Bouton, A., Simon, Y., Goussard, F., Teresi, L., Sansalone, V., 2017. New finite element study protocol: clinical simulation of orthodontic tooth movement. Int. Orthod. 15 (2), 165–179.
Cai, Y., Yang, X., He, B., Yao, J., 2015. Finite element method analysis of the periodontal ligament in mandibular canine movement with transparent tooth correction treatment. BMC Oral. Health 15, 106.
Christopher, A.G.M., Lekic, P., Marc, D.M., 2000. Role of physical forces in regulating the form and function of the periodontal ligament. Periodontology 24 (1), 56–72.
Cuoghi, O., Tondelli, P., Aiello, C., Mendonca, M., Costa, S., 2013. Importance of periodontal ligament thickness. Braz. Oral. Res 27 (1), 76–85.
Danz, J.C., Bibby, B.M., Katsaros, C., Stavropoulos, A., 2016. Effects of facial tooth movement on the periodontium in rats: a comparison between conventional and low force. J. Clin. Periodontol. 43 (3), 229–237.
Dorow, C., Sander, F.G., 2005. Development of a model for the simulation of orthodontic load on lower first premolars using the finite element method. J. Orofac. Orthop./Fortschr. der Kieferorthop. 66 (3), 208–218.
Er, Ö., Yaman, S.D., Hasan, M., 2007. Finite element analysis of the effects of thermal obturation in maxillary canine teeth. Oral. Surg., Oral. Med., Oral. Pathol., Oral. Radiol., Endodontology 104 (2), 277–286.
Field, C., Ichim, I., Swain, M.V., Chan, E., Darendeliler, M.A., Li, W., Li, Q., 2009. Mechanical responses to orthodontic loading: a 3-dimensional finite element multi-tooth model. Am. J. Orthod. Dentofac. Orthop. 135 (2), 174–181.
Heidary, Z., Mojra, A., Shirazi, M., Bazargan, M., 2018. A novel approach for Early Evaluation of orthodontic process by a Numerical thermo-mechanical analysis. Int J. Numer. Meth Biomed. Engng 34, e2899.
Huanga H., Tanga W., Yanb B., Wuc B., 2012. Mechanical responses of periodontal ligament under a realistic orthodontic loading. International Conference on Advances in Computational Modeling and Simulation, Procedia Engineering 31:828–833.
Jiang, N., Guo, W., Chen, M., et al., 2016. Periodontal ligament and alveolar bone in health and adaptation: tooth movement. Front. Oral. Biol. 18, 1–8.
Kawarizadeh, A., Bourauel, C., Jäger, A., 2003. Experimental and numerical determination of initial tooth mobility and material properties of the periodontal ligament in rat molar specimens. Eur. J. Orthod. 25 (6), 569–578.
Li Z., Gan Y., Xiong J., Tan J., Xia Z., Zhao Q., 2014. Modal analysis of a tooth-PDL-bone complex. IEEE International Conference on Information Science and Technology (ICIST) 4:772-775.
Liao, Z., Chen, J., Li, W., Darendeliler, M.A., Swain, M., Li, Q., 2016. Biomechanical investigation into the role of the periodontal ligament in optimising orthodontic force: a

finite element case study. Arch. Oral. Biol. 66, 98–107.
Maruo, I.T., Maruo, H., Saga, A.Y., de Oliveira, D.D., Argenta, M.A., Tanaka, O.M., 2016. Tridimensional finite element analysis of teeth movement induced by different headgear forces. Prog. Orthod. 17 (1), 1–9.
McCormack S.W., Witzel U., Watson P.J., Fagan M.J., Gröning F., 2014. The Biomechanical Function of Periodontal Ligament Fibres in Orthodontic Tooth Movement. Agarwal S. , ed. PLoS ONE 9(7):102387.
Nakajima, A., Murata, M., Tanaka, E., et al., 2007. Development of three-dimensional FE modeling system from the limited cone beam CT images for orthodontic tipping tooth movement. Dent. Mater. J. 26 (6), 882–891.
Oskui, I.Z., Hashemi, A., 2016. Dynamic tensile properties of bovine periodontal ligament: a nonlinear viscoelastic model. J. Biomech. 49 (5), 756–764.
Provatidis, C.G., 2000. A comparative FEM-study of tooth mobility using isotropic and anisotropic models of the periodontal ligament. Med. Eng. Phys. 22 (5), 359–370.
Qian, L., Todo, M., Morata, Y., Matsoshita, Y., Koyano, K., 2009. Deformation analysis of the periodontium considering the viscoelasticity of the periodontal ligament. Dent. Mater. 25 (10), 1285–1292.
Sameshima, G.T., Sinclair, P.M., 2001. Predicting and preventing root resorption: Part II. Treatment factors. Am. J. Orthod. Dentofac. Orthop. 119 (5), 511–515.
Storey, E., 1973. The nature of tooth movement. Am. J. Orthod. 63 (3), 292–314.
Su, M.Z., Chang, H.H., Chiang, Y.C., et al., 2013. Modeling viscoelastic behavior of periodontal ligament with nonlinear finite element analysis. J. Dent. Sci. 8 (2), 121–128.
Toms, S.R., Dakin, G.J., Lemons, J.E., Eberhardt, A.W., 2002. Quasilinear viscoelastic behavior of the human periodontal ligament. J. Biomech. 35 (10), 1411–1415.
Viecilli, R., Burstone, C., 2015. Ideal orthodontic alignment load relationships based on periodontal ligament stress. Orthod. Craniofac Res 18 (S1), 180–186.
Zargham, A., Rouhi, G., Geramy, A., 2016. Evaluation of long-term orthodontic tooth movement considering bone remodeling process and in the presence of alveolar bone loss using finite element method. Orthod. Waves 75 (4), 85–96.

Ms. Afsaneh Mojra has obtained her BSCE degree in Mechanical Engineering from Sharif University of Technology, Tehran, Iran in 2004, her MSC in Biomedical Engineering from Amirkabir University of Technology (Tehran Polytechnic), Tehran, Iran in 2006 and her PHD in Biomedical Engineering from Amirkabir University of Technology (Tehran Polytechnic), Tehran, Iran in 2011. She has spent a sabbatical position in the Biomedical Department, Eindhoven University of Technology, Netherlands in 2010. She is now an assistant professor in K. N. Toosi University of Technology in the Mechanical Engineering Department.

Mr. Mehdi Fakhimi Bonab is now a MSC student in Mechanical Engineering in K. N. Toosi University of Technology, Tehran, Iran.